Agglomeration during Precipitation: I. Tracer Crystals for $Al(OH)_3$ Precipitation

D. Ilievski and E. T. White
Dept. of Chemical Engineering, University of Queensland, St. Lucia, Queensland, 4072, Australia

Tracer crystals are developed to study the agglomeration, growth and residence time behavior of gibbsite crystals, an industrially important polymorph of $Al(OH)_3$, in continuous and batch precipitation. Satisfactory tracer crystals contain detectable amounts of Zn and have the crystal structure of gibbsite. The tracer crystals behave in the same manner during precipitation as the nontracer $Al(OH)_3$ crystals. The application of the tracer crystals for investigating, both batch and continuous, seeded $Al(OH)_3$ precipitation is demonstrated. The tracer experiments provide information on the growth and agglomeration kinetics of different size fractions. The tracers are a useful tool for the quantitative investigation of solid-phase residence time distributions within a crystallizer.

Introduction

Precipitation is an important operation in many industrial processes. For many operations, the size distribution of the product crystals is specified. The product crystal-size distribution produced depends on the precipitation processes (that is, crystal growth, agglomeration, nucleation, breakage and growth dispersion) and operating parameters (such as the residence time distribution). Optimization of the precipitation plant is often difficult because the precipitation mechanisms, particularly crystal agglomeration, are poorly understood. Useful information on the precipitation mechanisms and the residence time of particles in continuous or batch crystallizers might be obtained using tracer particles, which behave identically to the other particles in the system. The proposed application is analogous to that used for the analysis of chemical reactors with tracer chemicals (Levenspiel, 1972). In the current application, the agglomeration behavior, growth and residence time information may be deduced by monitoring the amounts of tracer particles appearing in the different size fractions of the product, at various times after addition to the crystallizer.

The precipitation system studied here is part of the commercially important Bayer process. The precipitation of gibbsite, a polymorph of $Al(OH)_3$, is a central step in the processing of bauxite to alumina. The mechanisms of crystal growth, agglomeration and nucleation have been observed to occur in these precipitators. Crystal agglomeration is the predominant size-enlargement mechanism and is the least understood.

Yamada and Yoshihara (1978) report using gallium doped $Al(OH)_3$ crystals to study the batch precipitation of $Al(OH)_3$ crystals in caustic aluminate. They do not describe how the crystal doping was performed nor do they demonstrate that these doped crystals have the same properties as the ordinary $Al(OH)_3$ crystals during precipitation. Further, gallium often naturally occurs in bauxite deposits and may be present as an impurity in Bayer process $Al(OH)_3$.

This article describes the successful development of tracer crystals that are shown to behave identically to ordinary gibbsite crystals during precipitation and that are easy to detect. The application of these tracers to the study of batch and continuous crystallization is demonstrated. The quantitative analysis of the tracer data is discussed in Part II of this article.

Tracer Selection Criteria

The prerequisites of an ideal solid's tracer for this work are:

(1) The tracer particles must behave identically to the other gibbsite particles in the system. The surface charge and composition of the tracer particles should be that of pure gibbsite so as not to affect growth rates or flocculation behavior.

(2) The identifying substance in the tracers must be distinct from the crystal material and easily detectable. It should

Current address of D. Ilievski: A. J. Parker Co-operative Research Centre for Hydrometallurgy, CSIRO Division of Minerals, P.O. Box 90, Bentley, Perth, Australia.

not be a material likely to be present as an impurity in the gibbsite initially used as seed or subsequently deposited.

(3) The substance must be inert; that is, it must not retard or enhance the precipitation processes to be studied.

(4) The hydrodynamic behavior of the tracer particles should be the same as that of the gibbsite particles.

(5) The identifying substance should be evenly distributed throughout each tracer particle.

Tracer Selection

The method adopted for manufacturing the tracers consisted of two steps. The first step was to coprecipitate gibbsite and a second material. The second step was to grow gibbsite on the surface of the coprecipitate to a thickness in excess of 5 microns. In this way the tracer species was imbedded and would not affect surface properties. The task of tracer selection then becomes one of determining a suitable second precipitate.

There are several mechanisms by which coprecipitation can occur, that is, surface adsorption, mechanical entrapment, solid solution, and post-precipitation. To make it easier to grow a uniform layer of pure gibbsite in the second step, the coprecipitate should retain the crystal structure of gibbsite. Thus it was considered desirable for the second material to be in solid solution within a matrix of gibbsite.

Pauling (1960) describes the principles that underlie the formation and stability of ionic or coordination compounds. To select a suitable chemical species for solid solution in gibbsite, it is necessary to know the structure and chemistry of gibbsite. On the atomic scale, gibbsite's structure consists of negatively charged sheets of hydroxyl ions. Each alternative pair of sheets is bound together by the Al ions. The aluminum ions occupy two-thirds of the available octahedral sites between the packed arrangement of hydroxyl layers (Misra, 1970; Giese, 1976; Pearson, 1955). For the ionic crystal structure to be stable, the cation (such as Al^{3+}) must be in contact with all the anions (that is, OH^-) surrounding it (Jaffe, 1988; Barrett et al., 1973; Flinn and Trojan, 1975; Adams, 1973). Thus any cation filling one of the octahedral sites between the hydroxide layers in gibbsite, by substitution of the Al^{3+} or entering a vacant site, must be large enough to not "rattle" around among the six OH^- ions surrounding the site, nor should it be so big as to cause excessive lattice deformation.

Gibbsite has a coordination number of six; that is, the Al ion is surrounded by six OH^- ions. Thus cations that have ionic radii such that the cation to OH^- radius ratio is between 0.732 and 0.414 are capable of a stable occupation of the octahedral sites in gibbsite (Jaffe, 1988; Barrett et al., 1973; Flinn and Trojan, 1975; Adams, 1973). The ionic radius of the hydroxyl ion is 1.32 Å (Shannon, 1976) and Table 1 lists some of the cations that have radii satisfying the above requirement.

Besides the geometric considerations discussed above, the candidate for replacing the Al^{3+} in the lattice, or filling the vacant interstitial sites, should have similar chemical properties to aluminum. These properties are strongly dependent on the number of electrons in the outer shell (columns of the periodic table) and the number of shells (rows of the periodic table).

Table 1. Ionic Radii of the Candidate Cations (after Shannon, 1976)

Cation	Ionic Radius Å	Coord. No.	Cation to Hydroxyl Ion Ratio
Al^{3+}	0.54	vi	0.41
Fe^{3+}	0.55	vi	0.42
Ga^{3+}	0.62	vi	0.47
Cr^{3+}	0.64	vi	0.48
Co^{2+}	0.65	vi	0.49
Mg^{2+}	0.72	vi	0.54
Zn^{2+}	0.74	vi	0.56

The incorporation of foreign ions in the interstices should be such that charge neutrality is maintained. For example, the incorporation of a divalent cation into gibbsite must be accompanied by the formation of a hydroxyl vacancy. Alternatively every pair of Al^{3+} ions substituted must be replaced by three divalent cations to ensure charge neutrality, or two divalent and two monovalent cations. Similar considerations apply for cations of all valences.

A number of elements satisfy most of the above requirements. The elements which may form solid solutions in gibbsite, due to their proximity to Al^{3+} on the periodic table and suitable ionic radii, are Ga, Mg, Zn, Fe, Cr and Co. On the basis of the above considerations gallium appears to be the most promising candidate. However, gallium often naturally occurs with aluminum in bauxite deposits and thus may already be present in some gibbsite as an impurity.

Tracer Manufacture

The tracers were manufactured in two steps. The procedure by which the tracers were manufactured is described in the following sections.

Step 1: coprecipitation

The first stage of tracer manufacture involved the coprecipitation of a second substance with $Al(OH)_3$. The coprecipitation experiments were performed using Co(II), Zn, Fe(III) or Mg as the second metal ion because they were immediately available. No coprecipitation experiments were performed using Ga or Cr.

In each case, the aqueous metal ion solutions were prepared by dissolving their chlorides in distilled water and filtering through a 0.22-μm membrane filter. On mixing the aqueous metal ion solutions with supersaturated caustic aluminate solution, also filtered at 0.22 μm, a precipitate formed immediately. These precipitates were filtered, washed, and analyzed by atomic absorption spectrometry. All the coprecipitates were found to contain both the second metal and Al.

The coprecipitation experiments were conducted in 1-L stainless-steel, stirred, baffled vessels. The temperature was controlled at 78°C to avoid the nucleation of separate $Al(OH)_3$ nuclei (Misra, 1970; Brown, 1975).

X-ray diffraction patterns of the coprecipitates were obtained using a Philips X-ray diffraction analyzer. The JCPDS-ICDD (1988) powder diffraction data file was searched to identify each coprecipitate by matching their

Table 2. Analysis of Final Coated Precipitate

Size Fraction (μm)	Bulk Analysis (Mass %)		Surface Analysis (Mole Ratio w.r.t. Al)	
	Al	Zn	Al	Zn
21–14	30.4	1.00	1.00	0.014
14–7.5	30.3	1.03	1.00	0.020
−7.5	24.0	21.1	—	—

diffraction patterns with those of known compounds, using the PC-PDF computer system. No matches were found for either the Zn(II)-Al(III), Co(II)-Al(III) or the Fe(III)-Al(III) coprecipitates. A possible match listed for the Mg(II)-Al(III) coprecipitate was with gibbsite.

Step 2: coating the coprecipitate with $Al(OH)_3$

The second stage of tracer development was to grow a uniform layer of $Al(OH)_3$ around the coprecipitates. The coating experiments were performed by adding the coprecipitates as seed to the 1-L stainless steel, stirred batch crystallizers containing supersaturated caustic aluminate solution. The crystallizers were operated at 78°C to minimize the nucleation of $Al(OH)_3$. Both Misra and White (1971) and Loh (1988) suggest that high seed surface areas favor the generation of nuclei in caustic aluminate solutions, so the seed charges were kept small (5–15 kg/m^3). This is much lower than industrial $Al(OH)_3$ precipitators where the seed addition is between 50 and 300 kg/m^3.

At the conditions of the $Al(OH)_3$ coating experiments, the induction time was estimated to be between 30–60 min, using the correlation proposed by Ilievski et al. (1989). The initial growth rates in the batch crystallizers were between 2 and 4.5 μm/h, and so a moderately rapid coverage could be expected. The intention was to grow the tracers to 10–20 μm. Growth rates for this system were measured using the procedure described by Misra and White (1971). A correlation for growth rates (Ilievski and White, 1994) was used to help plan the experiments.

The growth experiments on both the Fe(III)-Al(III) and Co(II)-Al(III) coprecipitates were considered unsuccessful because microscopic examination of the coated product particles showed that the $Al(OH)_3$ coating was not uniform. No further tracer crystal development work was done with these coprecipitates.

The preliminary coating experiments on the Zn(II)-Al(III) and Mg(II)-Al(III) coprecipitates gave a product which under microscopic examination appeared uniform. Analysis of the surface of these coated coprecipitate crystals using a Perkin-Elmer PHI model 560 ESCA/SAM/SIMS multi-technique surface analysis system showed approximately one Zn (or Mg) atom for every nine Al atoms, which was considered too high. It was found that by washing the Zn(II)-Al(III) coprecipitate in aqueous ammonia (28%) prior to coating, a satisfactory tracer crystal could be manufactured. It is presumed that the ammonia wash removed the Zn compounds from the surface of the coprecipitate. The dissolution of zinc hydroxide by aqueous ammonia is well documented in literature (Heslop and Jones, 1976; Cotton and Wilkinson, 1980).

The final Zn(II)-Al(III) tracers were classified into separate size fractions using a Warman Cyclosizer. The -7.5μm size fraction was not considered further. For the remaining fractions, the surface analyses of Table 2 show that there is approximately one Zn atom on the surface for every 100 Al atoms. The tracers contain 1% Zn by weight. Washing these new coated crystals with ammonia, however, did not significantly reduce the amount of Zn on the surface. These tracers were found to be satisfactory and no further experiments were conducted with other potential second metal ions.

Appraisal of Manufactured Tracer Crystals

Tracer crystal structure

The Jungner XDC-700 Guinier-Hagg powder diffraction camera was used to generate the diffraction pattern of the final Zn-Al tracer crystals. The Micro Powder Diffraction Search Match program identified gibbsite as the dominant phase with perhaps some bayerite present.

Tracer hydrodynamic behavior

Using a density bottle, the density of the tracers was found to be 2.439 g/ml at 23°C. Misra (1970) reports that the density of gibbsite is 2.424 g/mL. The denser tracer crystals would have a Stokes terminal settling velocity that is approximately 1% greater than an equivalent gibbsite particle. SEM micrographs show the tracer crystal habits to be indistinguishable from the gibbsite seed. Thus, the hydrodynamic behavior of tracer and gibbsite particles of the same size is unlikely to be significantly different.

Zn on the surface

Table 2 shows that the proposed Zn(II)-$Al(OH)_3$ crystals have one or two Zn atoms for every 100 Al atoms on the surface. This was considered acceptable.

Zn distribution in tracer crystals

It is necessary to know if the Zn is distributed uniformly among all the tracer particles or if the Zn is concentrated in a small number of the tracer particles. This was investigated by EDS, that is, generating X-ray maps of cross-sectioned tracer particles using a Tracor-Northern Series II 5502 X-Ray Microanalysis system. A distribution map for elemental Zn and Al for a group of tracer crystals showed that Zn and Al are present together in most particles. There were no particles that were purely Zn compounds containing no Al. In a very few particles, no Zn was detected. This does not necessarily mean that Zn was absent from the particle. It may be that the amount of Zn present was too small for detection. Alternatively, as the electron beam only excites the first 1–2 μm below the surface of the cross-sectioned particles, the Zn may be present at depths in the particle beyond detection.

Comparison of tracer agglomeration behavior with "normal" $Al(OH)_3$ particles

Two experiments were performed to determine whether the precipitation behavior of the tracers was different from ordinary gibbsite crystals:

(1) A preliminary batch precipitation was performed to determine if the tracer crystals agglomerate. The crystallizer was

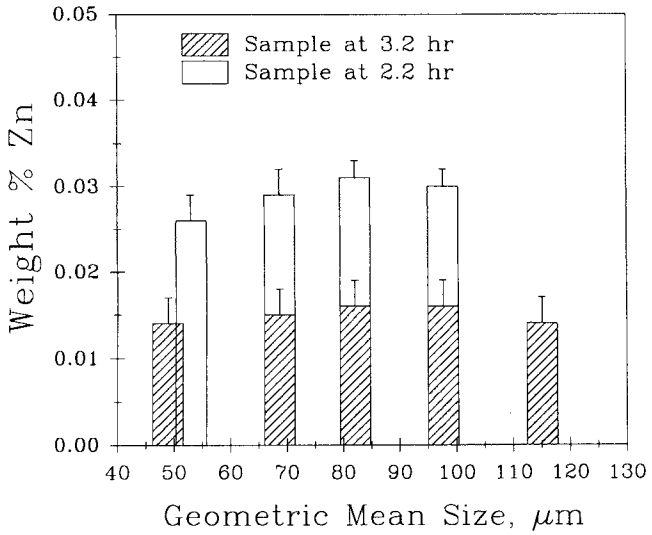

Figure 1. Distribution of the Zn tracer during batch precipitation.

Uniform distribution indicates that the tracers behave as the nontracer seed.

operated at conditions favorable for growth and agglomeration only. The Zn(II)-Al(III) tracer was added together with "normal" gibbsite seed crystals. The ratio of tracer to "normal" gibbsite was 1:4; both were from a $-14.7/+7.5$ μm sized fraction. Precipitation was conducted for 3 h in a 1-L, stainless-steel, baffled crystallizer. The particle sampling techniques yielded representative samples (Ilievski, 1991). All the final precipitate was found to be greater than 45 μm and contained zinc. The growth kinetics are slow, approximately 3 μm/h, for the precipitation conditions employed. Consequently, it was not possible for the tracer crystals to have grown to a size greater than 45 μm by molecular growth alone; hence, the tracer particles must have agglomerated.

(2) A second experiment was performed to demonstrate that the tracer particles agglomerate and grow in the same way as the gibbsite seed particles. This time the seeded precipitation experiment was performed in a 2.5-L batch crystallizer fitted with a draft tube. Tracers of size $-21/+10$ μm were added with the $Al(OH)_3$ seed of the same size in a 1:10 proportion. Slurry samples were taken from the crystallizer at various times. The solids were separated by filtration at 0.22 μm, washed in distilled water and wet screened with stainless-steel screens. The results shown in Figure 1 indicate that the Zn is evenly distributed among the size fractions. The tracer particles appear with equal probability in each size fraction indicating that they behave in the same way as "normal" gibbsite crystals of the same size, during precipitation.

Tracer Experiments

Continuous precipitator operation

Continuous precipitation experiments were performed in a continuously seeded crystallizer. A diagram of the experimental equipment is given in Figure 2. The 2.5-L stainless-

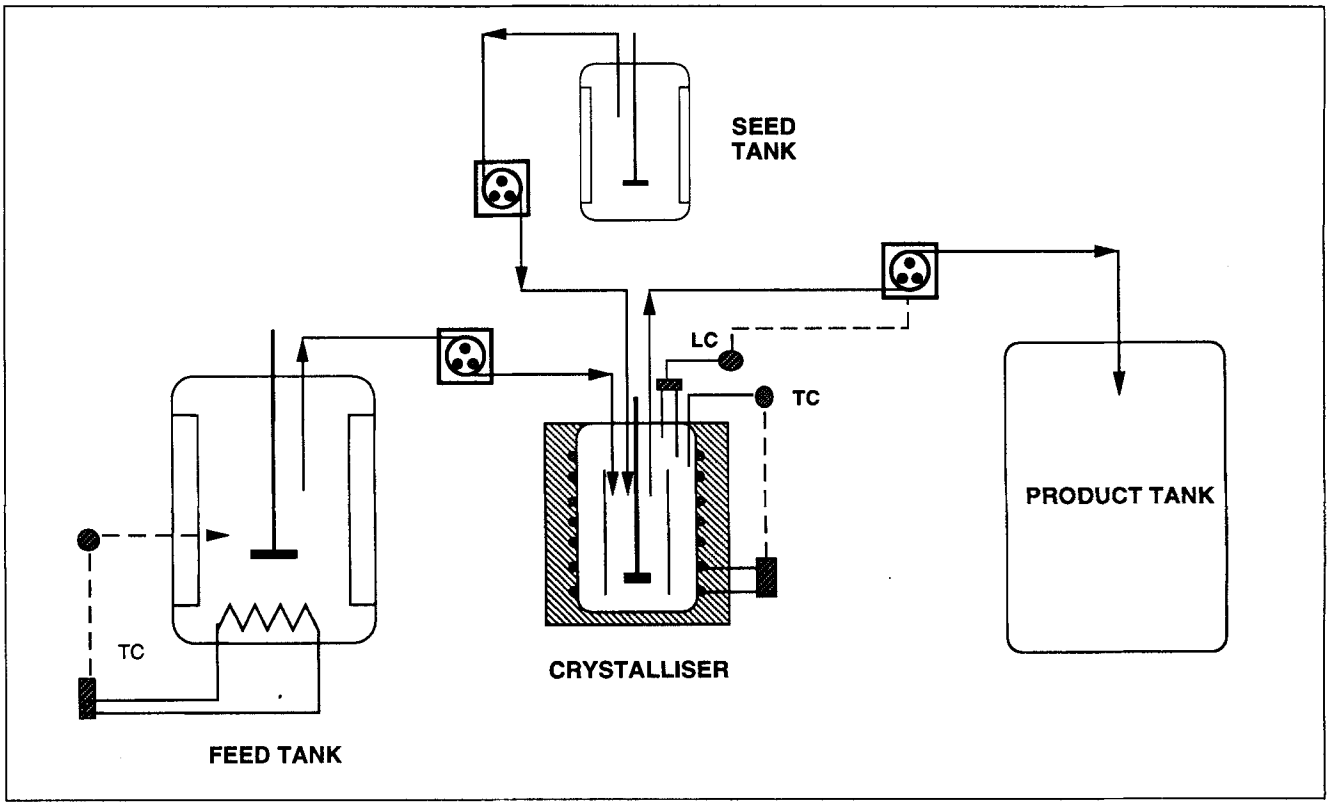

Figure 2. Continuous precipitator.

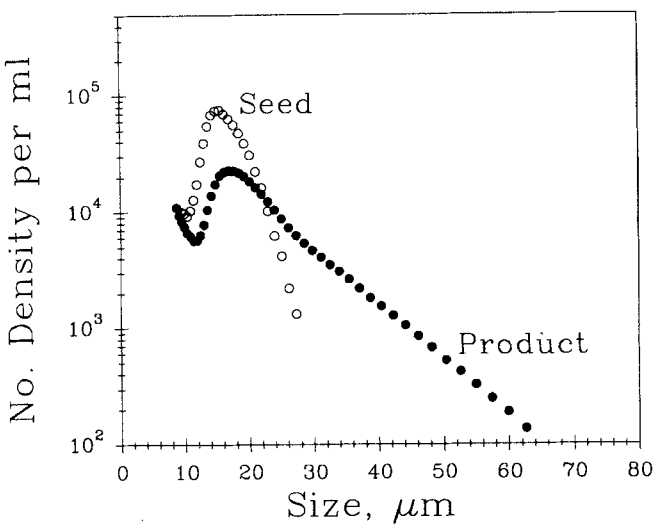

Figure 3. Steady-state crystal-size distribution for one of the precipitation experiments.

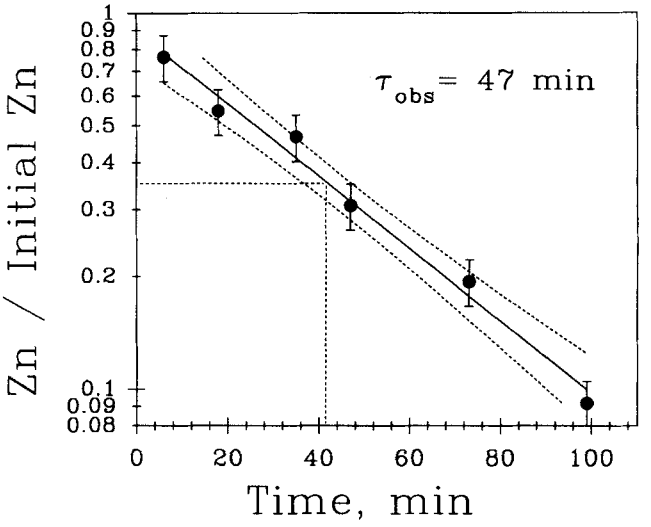

Figure 4. Residence time distribution of tracers.

steel crystallizer was fitted with a draft tube. The agitation conditions in the crystallizer were selected to be favorable for agglomeration, that is, complete suspension of the crystals and minimum shear forces in the fluid (Ilievski and White, 1994). The agitation power per unit volume for the experiments was 21 $W \cdot m^{-3}$. Supersaturated caustic aluminate feed solution at 103–108°C was fed into the draft tube region of the crystallizer, as recommended by Randolph and Larson (1988) to ensure rapid mixing. The seed slurry stream, containing less than 5% solids, was also directed into this region. The crystallizer was controlled at 78°C to avoid nucleation and to minimize induction times (Ilievski et al., 1989). The seed crystals were the gibbsite polymorph of $Al(OH)_3$. The seed particle-size distribution (PSD), prepared by classification with a Warman Cyclosizer, were narrow and well defined.

Steady-state operation was verified by observation of the product PSD and solids content. The size distributions were measured with an Elzone Celloscope 280PCXY. The steady-state product PSD from one of the continuous precipitation experiments is given in Figure 3. Component mass balances on $Al(OH)_3$ and Na_2O were found to be consistent within experimental error. The number of crystals present at steady state was lower than the number of seed crystals added, indicating that agglomeration has occurred. Scanning electron micrographs of the steady-state product crystals from the experiments also showed evidence of agglomeration. For the operating conditions employed, crystal growth and agglomeration are the dominant size-enlargement mechanisms present.

Tracer addition during continuous operation

A quantity of tracer crystals, with the same size distribution as the seed (that is, the same size fraction cut from the Warman Cyclosizer), was added as an impulse to the crystallizer at steady state. Slurry samples were then taken from the product stream at different times after the tracer addition. The slurry samples were filtered at 0.22 μm and repeatedly washed. The filtered solids samples were then wet screened using stainless-steel sieves, ranging in size from 38 to 125 μm. The size fractions were analyzed for Zn by atomic absorption spectroscopy. Tracer experiments were performed during three separate continuous precipitation runs.

Figure 4 is a residence time distribution plot for one of the runs. It shows the variation with time of the total Zn content in the solids, expressed as a fraction relative to the amount of Zn initially added. All such plots showed the Zn concentration of the exit solids to be exponentially distributed with time, as would be expected for perfectly mixed vessel with representative overflow. This is consistent with the finding of Ilievski (1991), who showed that the same crystallizer vessel behaves as a perfectly mixed vessel with respect to the solids for the same agitation conditions reported here. Ilievski also shows, using aqueous KCl as the tracer, that the liquid phase is perfectly mixed. The mean of the exponential tracer distribution, 42 ± 6 min (marked by the vertical dotted line on Figure 4) agrees with the experimentally measured fluid mean residence time of 47 ± 2 min. There was agreement between the experimental mean residence time and the mean of the tracer distributions for all three tracer experiments performed. These results illustrate the applicability of tracer crystals as a tool to study the residence time distribution of the solids in a precipitator with growth and agglomeration occurring.

Figure 5 shows the fraction of zinc distributed between the various size fractions. This plot gives information on the rate at which the tracers grow and/or agglomerate into or out of a size range. Since the tracers are representative of the other seed crystals, this represents the behavior of all the seed crystals. The ordinate for this plot is the ratio of the mass of Zn in the size fraction to the total mass of Zn in the product at the sample time. The number of size fractions that can be reported depends on the available sample volume and the classification technique.

For all three experiments in the first 10 to 20 min, the amount of tracer in the -38 μm range remained constant with little appearance of tracers in the larger sizes. This could

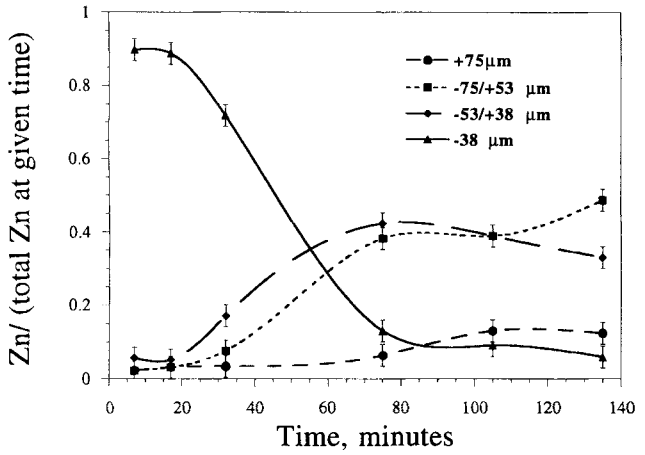

Figure 5. Distribution in Zn concentration with time in each size interval for one of the continuous precipitation experiments.

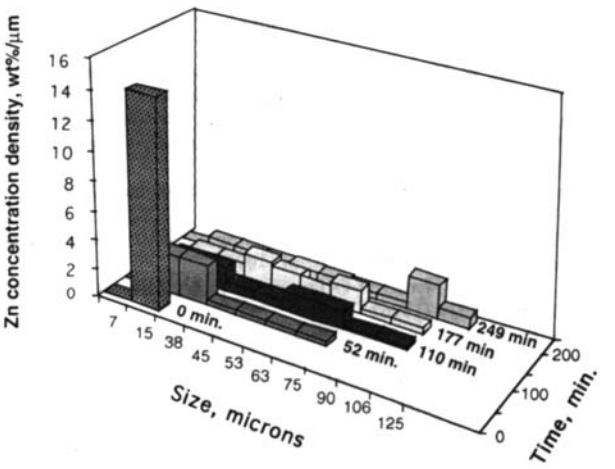

Figure 6. Distribution of Zn with size and time for a batch precipitation experiment.

be the result of tracers mainly agglomerating with small particles, so that the agglomerate does not appear in the larger size fractions. The use of micro-mesh sieves for future experiments may clarify the situation. After this initial period, the tracers are detected in size fractions into which they could only have reached by agglomeration, since the linear crystal growth rate (between 2 and 5 μm/h) is slow. The task of inferring precipitation kinetics, particularly the agglomeration kinetics, is the topic of Part II of this article.

Tracer addition during batch precipitation

The batch experiments described earlier demonstrated that the tracers behave as "normal" gibbsite. Further batch tracer experiments were performed to establish what type of information this technique can supply on precipitation mechanisms. Gibbsite seed, with a bi-modal size distribution, and tracer particles were added simultaneously to a batch precipitator containing supersaturated caustic aluminate solution. Slurry samples were taken at different times during the precipitation. The solids were filtered, washed, and wet screened with stainless-steel screens. The solids were then dissolved in acid and analyzed for Zn.

Figure 6 shows the results of a tracer experiment on a batch precipitator. For the reported experiment, the bi-modal seed was prepared by combining the $-14.7/+7$ and $-35/+20$ μm particle size cuts from the Warman Cyclosizer. Tracer particles were also sized $-14.7/+7$ μm. Figure 6 shows the distribution of Zn as a function of size (represented as a histogram) measured at five separate times. The figure shows how the tracer particles, and hence the seed particles of the same size, are distributed with time. Three important qualitative observations that are immediately evident from the tracer data in this figure are:

(1) There is clear evidence of agglomeration, as Zn is detected in size fractions into which the tracers could not have grown due to the slow growth kinetics of this system (≤ 3 μm/h).

(2) Particles as large as 60 μm do agglomerate. This is contrary to the expectation that the maximum agglomerate size should be approximately the same as the Kolmogoroff microscale of turbulence (Mullin, 1993; Söhnel and Garside, 1992; Akers et al., 1987), which is approximately 13 μm for the current experiments. An upper limit on agglomerate size was incorporated into the $Al(OH)_3$ precipitator model of Steemson et al. (1984). Their model assumed maximum agglomerate sizes ranging from 5 to 40 μm, depending on the process conditions.

(3) In contrast to the findings of Yamada and Yoshihara (1978), who claim that fine particles (mean = 3 μm) agglomerate with other fine particles and do not agglomerate with coarse particles (mean = 50 μm), the results of this work indicate that small particles and large particles do agglomerate.

Conclusions

Tracer crystals suitable for $Al(OH)_3$ precipitation studies have been developed and successfully tested. The tracers contain 1% zinc, which allows individual tracer crystals to be identified by EDS or the average concentration using bulk Zn analysis (such as by Atomic Absorption).

The tracers were prepared using a two-step process of co-precipitation and coating. It was shown that the zinc is distributed among all tracer particles and the tracers behave like normal $Al(OH)_3$ crystals during precipitation.

Use of the tracer crystals allows the study of agglomeration mechanisms during precipitation. They can also be used to monitor the residence time distribution behavior of the solid phase in a crystallizer.

The tracer development technique outlined in this work is general and can be applied to other crystallization systems.

Acknowledgment

The authors gratefully acknowledge Comalco Central Research Laboratory, Thomastown, Australia, for funding the work through a PhD program. Thanks are due to CSIRO Australia for providing a postdoctoral fellowship enabling this work to be continued.

Literature Cited

Adams, D. M., *Inorganic Solids*, Wiley, New York (1973).
Akers, R. J., A. G. Rushton, and J. I. T. Stenhouse, "Floc Breakage: the Dynamic Response of the Particle Size Distribution to a Step

Change in Turbulent Energy Dissipation," *Chem. Eng. Sci.*, **42**, 787 (1987).
Barrett, C. R., W. D. Nix, and A. S. Tetelman, *The Principles of Engineering Materials*, Prentice-Hall, Englewood Cliffs, NJ (1973).
Brown, N., "A Quantitative Study of New Crystal Formation in Seeded Caustic Aluminate Solutions," *J. Cryst. Growth*, **29**, 309 (1975).
Cotton, F. A., and G. Wilkinson, *Advanced Inorganic Chemistry*, 4th ed., Wiley, New York (1980).
Flinn, R. A., and P. K. Trojan, *Engineering Materials and their Applications*, Houghton Mifflin, Boston (1975).
Giese, Jr., R. F., "Hydroxyl Orientations in Gibbsite and Bayerite," *ACTA*, **B32**, 1719 (1976).
Heslop, R. B., and K. Jones, *Inorganic Chemistry: A Guide to Advanced Study*, Elsevier, Amsterdam (1976).
Ilievski, D., "Modelling $Al(OH)_3$ Agglomeration During Batch and Continuous Precipitation in Supersaturated Caustic Aluminate Solutions," PhD Thesis, Univ. of Queensland, Australia (1991).
Ilievski, D., and E. T. White, "Agglomeration During Precipitation: Agglomeration Mechanism Identification for $Al(OH)_3$ Crystals in Stirred Caustic Aluminate Solutions," *Chem. Eng. Sci.*, **49**(19), 3227 (1994).
Ilievski, D., and E. T. White, "Customising a Laboratory Crystalliser for Agglomeration Studies," *Chemeca Proc. of Australasian Chem. Eng. Conf.*, p. 213 (1994).
Ilievski, D., S. G. Zheng, and E. T. White, "Induction Times for Growth in Seeded Supersaturated Caustic Aluminate Solutions," *Chemeca Proc. of Australasian Chem. Eng. Conf.*, p. 1012 (1989).
Jaffe, H. W., *Introduction to Crystal Chemistry*, Chap. 4, Cambridge Univ. Press, Cambridge (1988).
JCPDS-ICDD, *Powder Diffraction File*, International Centre for Diffraction Data, Swarthmore (1988).
Levenspiel, O., *Chemical Reaction Engineering*, 2nd ed., Wiley, New York (1972).
Loh, P. I. W., "Secondary Nucleation of Alumina Trihydrate in a Batch Crystalliser," M. Eng. Sci. Thesis, Curtin Univ. of Technology, Perth, Australia (1988).
Misra, C., and E. T. White, "Kinetics of Crystallisation of Aluminium Trihydroxide from Seeded Caustic Aluminate Solutions," *AIChE Symp. Ser.*, **67**(110), 53 (1971).
Misra, C., "The Precipitation of Bayer Aluminium Trihydroxide," PhD Thesis, Univ. of Queensland, Australia (1970).
Mullin, J. W., *Crystallisation*, 3rd ed., Butterworth-Heinemann, Oxford, p. 287 (1993).
Pauling, L., *The Nature of the Chemical Bond*, Chap. 13, 3rd ed., Cornell Univ. Press, Ithaca, NY (1960).
Pearson, T. G., *The Chemical Background to the Aluminium Industry, Lectures, Monographs, and Reports, No. 3*, Royal Inst. of Chemistry, London (1955).
Randolph, A. D., and M. A. Larson, *Theory of Particulate Processes*, 2nd ed., Academic Press, New York (1988).
Shannon, R. D., "Revised Effective Ionic Radii and Systematic Studies of Interatomic Distances in Halides and Chalcogenides," *ACTA Cryst.*, **A32**, 751 (1976).
Söhnel, O., and J. Garside, *Precipitation: Basic Principles and Applications*, Butterworth-Heinemann Ltd., Oxford, p. 191 (1992).
Steemson, M. L., E. T. White, and R. J., Marshall, "Mathematical Model of the Precipitation Section of a Bayer Plant," *Light Metals*, 237 (1984).
Yamada, K., and M. Yoshihara, "Crystallisation of Aluminium Trihydroxide from Sodium Aluminate Solution," *Light Metals*, 19 (1978).

Manuscript received Oct. 29, 1993, and revision received May 6, 1994.